

# High resolution $^{31}\text{P}$ NMR study of octacalcium phosphate

Yao-Hung Tseng,<sup>a,b</sup> Jinhua Zhan,<sup>a,b</sup> Kyle S.K. Lin,<sup>a</sup> Chung-Yuan Mou,<sup>a,b</sup>  
and Jerry C.C. Chan<sup>a,\*</sup>

<sup>a</sup> Department of Chemistry, National Taiwan University, No. 1, Section 4, Roosevelt Road, Taipei, Taiwan

<sup>b</sup> Center of Condensed Matter, National Taiwan University, No. 1, Section 4, Roosevelt Road, Taipei, Taiwan

Received March 12, 2004; revised May 21, 2004

## Abstract

We have assigned the  $^{31}\text{P}$  high-resolution spectrum of octacalcium phosphate by  $^{31}\text{P}$  double quantum and HETCOR spectroscopy. The  $^{31}\text{P}$  peaks at  $-0.2$ ,  $2.0$ ,  $3.3$  and  $3.7$  ppm are assigned to P5/P6, P3, P2/P4 and P1, respectively. Our data reveal that substantial amount of the  $\text{PO}_4^{3-}$  groups at the P2 and P4 sites have been transformed to  $\text{HPO}_4^{2-}$  in our octacalcium phosphate sample.

© 2004 Elsevier Inc. All rights reserved.

**Keywords:** Octacalcium phosphate; OCP; MAS; Double-quantum; HETCOR

## Introduction

Studies of calcium phosphates have been actively pursued for many years because of their importance in biomineralization. In particular, octacalcium phosphate (OCP) has received considerable attention because it is structurally related to hydroxyapatite (HAP), which is the major inorganic phase in the human body [1,2]. Over the years, it has been postulated that OCP is the precursor phase of HAP in calcified tissue [3]. Recently, the first experimental evidence for the presence of trace amount of OCP in a biological tissue is obtained by high-resolution electron microscopy [4]. This work marks an important advancement in the study of biomineralization. Nevertheless, it is not clear how OCP is transformed to HAP in biological matrix. It is therefore highly desirable to develop other physical techniques that can detect OCP in calcified tissues. OCP, which has a chemical formula of  $\text{Ca}_8(\text{HPO}_4)_2(\text{PO}_4)_4 \cdot 5\text{H}_2\text{O}$ , is thermodynamically unstable and will convert slowly to HAP,  $\text{Ca}_{10}(\text{PO}_4)_6\text{OH}_2$ , and monetite,  $\text{CaHPO}_4$ , at elevated temperature [5]. As such, solid-state NMR is well suited to characterize this meta-stable

material, in which other phases of calcium phosphate may coexist. In particular,  $^{31}\text{P}$  NMR is expected to be the perfect probe nucleus for OCP detection because there are six crystallographically non-equivalent phosphorous sites [1,6].

Considerable efforts have been made to investigate OCP by solid-state NMR. Some years ago, Yesinowski and Eckert had successfully applied  $^1\text{H}$  MAS-NMR to characterize the hydrogen environments of OCP, which provides evidence for the presence of hydroxyl groups in the so-called apatitic layer [7]. This assignment has been confirmed by other experiments such as  $^1\text{H}$  CRAMPS and ultra-fast MAS [8,9]. The first high-resolution  $^{31}\text{P}$  NMR study of OCP can be dated back to the 1980s [10]. The partially resolved  $\text{HPO}_4^{2-}$  and  $\text{PO}_4^{3-}$  signals are assigned by cross-polarization experiments with variable contact times. Similar results were obtained using the dipolar dephasing technique [11]. Later, another  $^{31}\text{P}$  NMR study of OCP was conducted at a magnetic field of  $2.35\text{ T}$  under MAS spinning of  $5\text{ kHz}$  [12]. The resolution is somewhat better and there are three peaks resolved. Based on the earlier results, the peaks at  $-0.2$  and  $3.3\text{ ppm}$  were assigned to  $\text{HPO}_4^{2-}$  and the apatitic  $\text{PO}_4^{3-}$  groups, respectively. The signal at  $2.2\text{ ppm}$  is assigned to the other  $\text{PO}_4^{3-}$  groups at the junction of the apatitic and hydrated layers. Recently, a  $^{31}\text{P}$  NMR

\*Corresponding author. Fax: +886-2-2363-6359.

E-mail address: [chanjcc@ntu.edu.tw](mailto:chanjcc@ntu.edu.tw) (J.C.C. Chan).

spectrum of OCP has been reported at 7.05 T and 9 kHz [13], which shows four well-resolved  $^{31}\text{P}$  resonances. Unfortunately, the authors did not make any assignment at all because it is not trivial to assign the  $^{31}\text{P}$  resonances based on the chemical shift data alone. Without a complete assignment of the  $^{31}\text{P}$  spectrum of OCP, it is premature to apply  $^{31}\text{P}$  NMR for the detection of OCP in biological tissues.

In this work, we demonstrate that  $^{31}\text{P}$  double-quantum spectroscopy and  $^{31}\text{P}\{^1\text{H}\}$  heteronuclear correlation (HETCOR) can be used to assign all the four resolved peaks of the  $^{31}\text{P}$  MAS spectrum measured at 7.05 T and 10 kHz. Our assignment will not only establish  $^{31}\text{P}$  NMR as a sensitive method for OCP detection, but also help facilitate the study of OCP to HAP transformation, which has been postulated as the mechanism for the formation of biological apatites [3].

## 2. Materials and methods

### 2.1. Sample preparation and characterization

Urea (99.5%), sodium phosphate monobasic dehydrate ( $\text{H}_2\text{NaPO}_4 \cdot 2\text{H}_2\text{O}$ ) (99%) and calcium nitrate tetrahydrate ( $\text{Ca}(\text{NO}_3)_2 \cdot 4\text{H}_2\text{O}$ ) (99%) were used as received (Acros). 10 mmol  $\text{Ca}(\text{NO}_3)_2 \cdot 4\text{H}_2\text{O}$ , 10 mmol  $\text{H}_2\text{NaPO}_4 \cdot 2\text{H}_2\text{O}$  and 20 mmol urea were dissolved in 400 ml doubly distilled water and then sealed in a polypropylene container. The aqueous solution was kept at 100°C for 3 h. The precipitates thus obtained were filtered, washed and then dried at 60°C for 1 day.

X-ray diffraction analysis was performed on a Philips X'Pert diffractometer, using  $\text{Cu-K}\alpha$  radiation ( $\lambda = 1.5418 \text{ \AA}$ ). The field emission scanning electron micrograph (FE-SEM) was taken on a JEOL-JSM-6700F field emission scanning electron microscope operating at 10 kV.

### 2.2. Solid-state NMR

All NMR experiments were carried out at  $^{31}\text{P}$  and  $^1\text{H}$  frequencies of 121.5 and 300.1 MHz, respectively, on a Bruker DSX300 NMR spectrometer equipped with a commercial 4 mm MAS-NMR probe. All spectra were measured at room temperature. The sample was confined to the middle  $\frac{1}{3}$  of the rotor volume using Teflon spacers. MAS frequency variation was limited to  $\pm 3 \text{ Hz}$  using a commercial pneumatic control unit. Chemical shifts were externally referenced to 85% phosphoric acid and TMS for  $^{31}\text{P}$  and  $^1\text{H}$ , respectively. The  $^{31}\text{P}$  spin-relaxation times ( $T_1$ ) were determined by the saturation-recovery technique. The pulse sequences used for the  $^{31}\text{P}$  double-quantum (DQ) experiment and  $^{31}\text{P}\{^1\text{H}\}$  HETCOR measurements are shown in Fig. 1.

$^{31}\text{P}$  DQ experiment was carried out under MAS spinning frequency of 6 kHz. Quadrature detection in the  $F_1$  dimension was achieved by the hypercomplex approach. For each  $t_1$  increment 64 transients were accumulated, and a total of 50 increments were done at steps of one rotor period. Recycle delay of 18 s was applied. To prepare the initial spin system identically for each transient, a saturation comb was applied prior the recycle delay. During the DQ excitation and reconversion periods, the  $^{31}\text{P}$  rf nutation frequency was set to 42 kHz. The standard four-step phase cycling of the excitation block was used to select the DQ coherence. Probe ringdown and dc offset artifacts are suppressed by inverting the phase of the reading pulse and alternating addition and subtraction of FID signals. Together with CYCLOPS our phase cycling has a total of 32 steps.

The heteronuclear correlation (HETCOR) spectrum of OCP is measured by  $^{31}\text{P}\{^1\text{H}\}$  cross polarization at a spinrate of 10 kHz. Recycle delay was set to 10 s. Contact time was set to 2.5 ms. During the contact time the  $^1\text{H}$  nutation frequency was set equal to 50 kHz and that of  $^{31}\text{P}$  was ramped through the Hartmann–Hahn matching sideband [14]. Other conditions were similar to

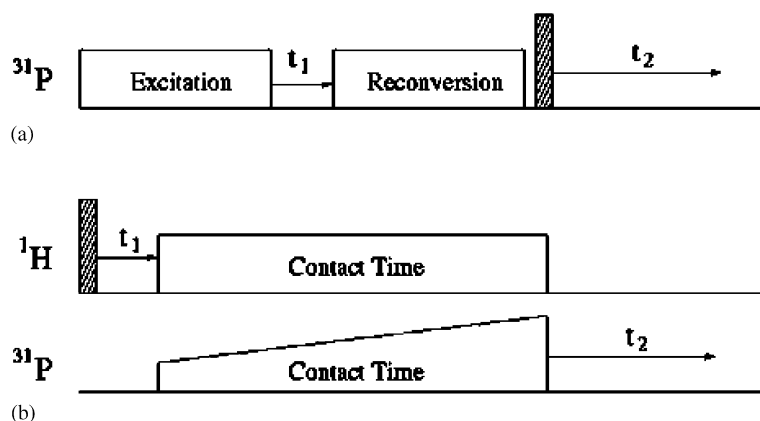


Fig. 1. Pulse sequences used for the (a)  $^{31}\text{P}$  double-quantum and (b)  $^{31}\text{P}\{^1\text{H}\}$  HETCOR measurements. The shaded rectangle denotes  $\pi/2$  pulse.

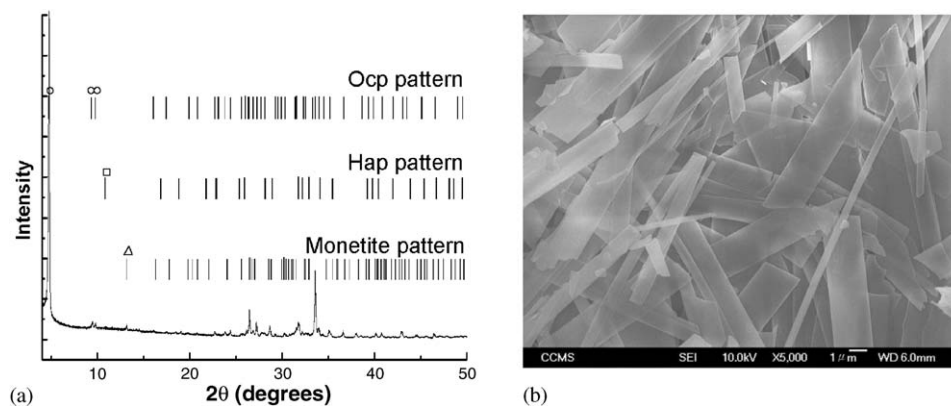


Fig. 2. (a) XRD pattern measured for the OCP sample; (b) SEM image of the OCP sample.

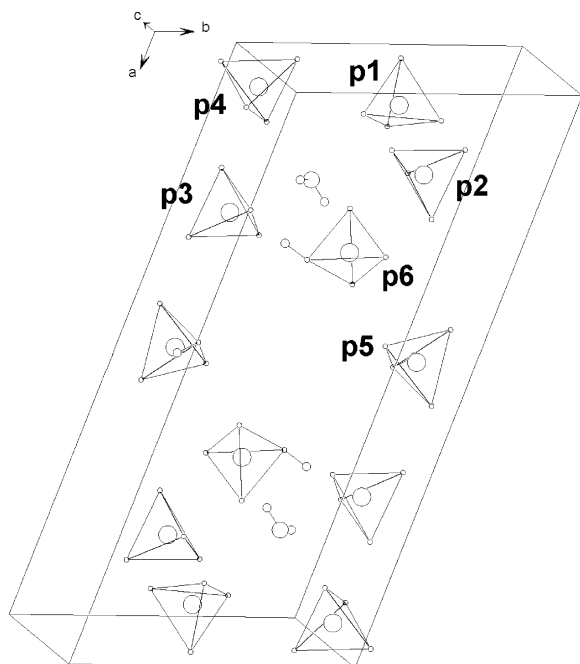


Fig. 3. Illustration of the unit cell of OCP. Among the 12 phosphorous sites only six of them are non-equivalent. The four  $\text{PO}_4^{3-}$  groups are labeled as P1–P4 and the two  $\text{HPO}_4^{2-}$  groups as P5 and P6. For simplicity all the water molecules are hidden except those corresponding to the OH sites of HAP.

those described in the DQ experiment. Spin-temperature inversion was incorporated with CYCLOPS, resulting in an eight-step phase cycling.

### 3. Results

#### 3.1. XRD and SEM

The XRD data measured for our OCP sample is shown in Fig. 2a. The calculated patterns for OCP, HAP and monetite are aligned with the experimental pattern for comparison. The absence of the reflection at  $2\theta = 10.8^\circ$  (the characteristic reflection of HAP) in the

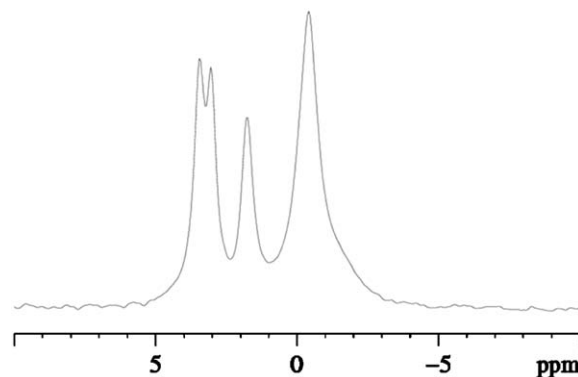


Fig. 4.  $^{31}\text{P}$  MAS spectrum of OCP measured at 10 kHz MAS spinning.  $^1\text{H}$  decoupling at 80 kHz was applied during acquisition. Recycle delay was set to 610 s.

experimental pattern indicates that our sample does not contain any identifiable HAP. On the other hand, a minor amount of monetite is present in our OCP sample. The SEM image of our OCP sample is shown in Fig. 2b. The morphology of the sample is uniform and the crystals typically have rectangular shapes.

For convenience, we have reproduced part of the crystallographic data of OCP in Fig. 3 [1]. Accordingly, there are six non-equivalent sites for phosphorus, in which P1–P4 are  $\text{PO}_4^{3-}$  groups while P5 and P6 are  $\text{HPO}_4^{2-}$  groups.

#### 3.2. Solid-state NMR

The  $^{31}\text{P}$  MAS spectrum of OCP is shown in Fig. 4. There are four resolved peaks positioned at  $-0.2$ ,  $2.0$ ,  $3.3$  and  $3.7$  ppm with intensity ratio equal to 3:1:1:1 approximately. The spin–lattice relaxation parameters of these peaks range from 89 to 123 s.

Our  $^{31}\text{P}$  double quantum (DQ) spectrum is obtained by the POST-C7 sequence [15–17]. The DQ spectrum shown in Fig. 5. has four sets of auto- and cross-correlation peaks. Referring to the structural information shown in Table 1, we can preliminarily assign the

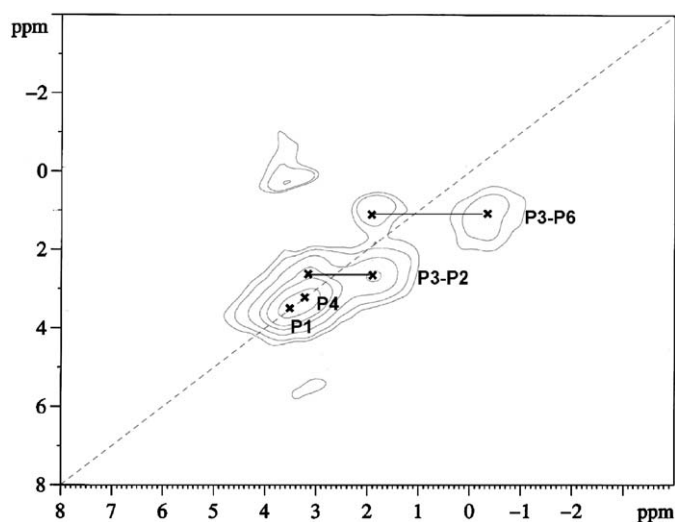


Fig. 5.  $^{31}\text{P}$  double quantum spectrum of OCP. P3–P6 and P3–P2 connectivities are identified by the cross-correlation peaks. P1–P1 and P4–P4 connectivities are indicated by the auto-correlation peaks labeled as P1 and P4, respectively.

Table 1

Summary of the OCP internuclear distances which are relevant to the analyses of  $^{31}\text{P}$  double quantum and  $^{31}\text{P}\{^1\text{H}\}$  HETCOR experiments. All the distances are reported in angstrom

$^{31}\text{P}$ DQ spectrum auto-correlation		$^{31}\text{P}$ DQ spectrum cross-correlation		$^{31}\text{P}\{^1\text{H}\}$ HETCOR <sup>a</sup>			
P1–P1	4.043	P2–P3	4.017	P6–O4	3.507	P2–H9	3.448
P4–P4	4.041	P3–P6	4.206	P4–O4	3.635	P4–H10	3.850
P5–P5	4.042	P5–P6	4.350	P2–O4	3.743	P2–H10	3.946
P2–P2	6.835	P1–P4	4.697	P6–O4	3.990	P4–H9	4.418
P3–P3	6.835	P1–P2	4.707	P1–O4	5.009	P3–H10	4.424
P6–P6	6.835	P2–P4	4.722			P1–H10	4.679
		P2–P6	4.951			P1–H9	5.164
		P1–P6	4.969				

<sup>a</sup>O(4), H(9) and H(10) correspond to the water molecule occupied at the OH site of HAP [1].

auto-correlation peaks at 3.3 ppm to P1 or P4. The same is true for the signal at 3.7 ppm. Unambiguous assignment can be made only when we incorporate the HETCOR data in our analysis (vide infra). Based on the positions of the cross-correlation peaks we can assign with certainty the resonances at 2.0 and 3.3 ppm to P3 and P2, respectively. The auto-correlation peak arising from P5 is not found in our DQ spectrum. Repeat measurement with proton decoupling at 80 kHz, our highest possible decoupling field, throughout the experiment gave the same result. Presumably the strong  $^1\text{H}$ – $^{31}\text{P}$  coupling for the  $\text{HPO}_4^{3-}$  species renders the DQ signal undetectable. The same argument also explains the missing of the P5–P6 cross-peak. On the other hand, the observation of the cross-correlation peak between P3 ( $\text{PO}_4^{3-}$ ) and P6 ( $\text{HPO}_4^{2-}$ ) shows that P6 may undergo rapid molecular motion in the NMR time scale, which substantially attenuates the  $^1\text{H}$ – $^{31}\text{P}$  coupling. This explanation is consistent with the earlier observation that the chemical shift anisotropy measured for  $\text{HPO}_4^{2-}$  in OCP increased when the temperature was lowered to  $-165^\circ\text{C}$  [10]. Furthermore, the single-crystal X-ray

diffraction study of OCP shows that there are six calcium ions surrounding P5 but only four  $\text{Ca}^{2+}$  for P6 [1]. Hence it is not unexpected that these two  $\text{HPO}_4^{2-}$  groups have different molecular motions. We note that the closest distance between P1 and P6 is 4.969 Å, which seems too large to give a detectable DQ signal in our experiment.

For comparison we append the  $^1\text{H}$  MAS spectrum next to the  $^1\text{H}$  projection of our  $^{31}\text{P}\{^1\text{H}\}$  HETCOR spectrum shown in Fig. 6. It has been established that the  $^1\text{H}$  signal at 0.18 ppm arises from the OH group [7,9], which is correlated to the  $^{31}\text{P}$  resonance at 3.3 ppm but not at 3.7 ppm. Referring to the structural data summarized in Table 1, P1 cannot account for the  $^{31}\text{P}$  signal correlated to the hydroxyl  $^1\text{H}$  signal. Together with the  $^{31}\text{P}$  DQ data, we can therefore assign the  $^{31}\text{P}$  signal at 3.7 ppm to P1, and the signal at 3.3 ppm to both P2 and P4. The relatively sharp  $^1\text{H}$  peak at 1.44 ppm has been previously assigned to the O(5) water molecule, which is rather isolated from all the  $\text{PO}_4^{3-}$  groups (closest distance 5.827 Å) [7]. The fact that this peak is not correlated to any  $\text{PO}_4^{3-}$  groups in our

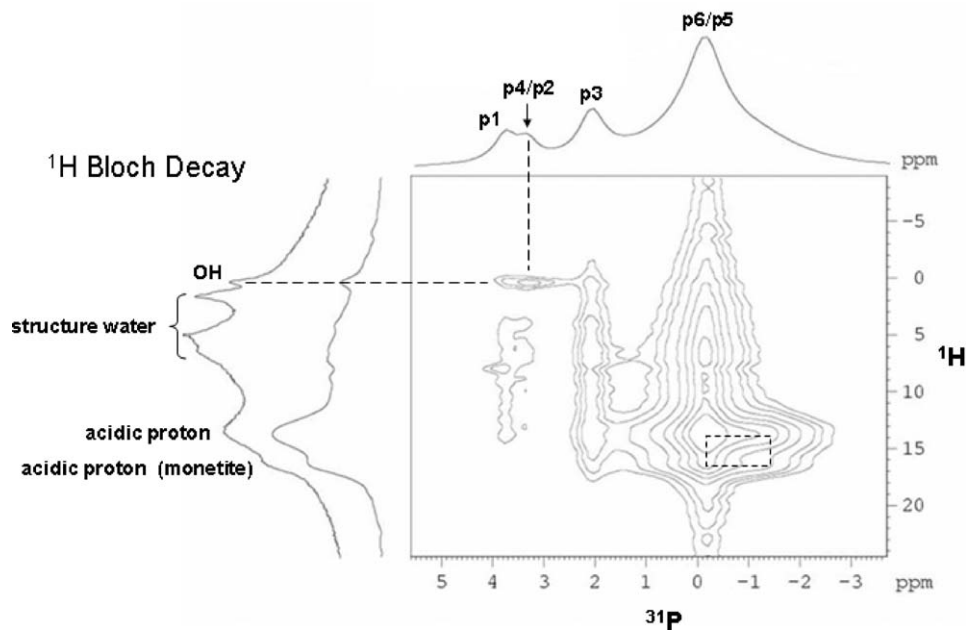


Fig. 6.  $^{31}\text{P}\{^1\text{H}\}$  HETCOR spectrum of OCP. Projections of the  $^{31}\text{P}$  and  $^1\text{H}$  dimensions are shown. For comparison the  $^1\text{H}$  MAS spectrum is appended next to the  $^1\text{H}$  projection spectrum. The vertices of the rectangular box correspond to the cross peaks of monetite. Note that the OCP signal also contributes to the cross peak at  $-0.2$  ppm ( $^{31}\text{P}$ ) and  $13.6$  ppm ( $^1\text{H}$ ).

HETCOR spectrum is consistent with this earlier assignment. As expected, the  $^{31}\text{P}$  peak at  $-0.2$  ppm (P5 and P6) is correlated to the  $^1\text{H}$  signals at  $5.5$  and  $13.34$  ppm, which have been assigned to the structural water and the acidic proton of  $\text{HPO}_4^{2-}$  [7]. Our XRD data shows that there is small amount of monetite present in our OCP sample. The  $^{31}\text{P}$  MAS spectrum of monetite measured by Rothwell et al. show two partially resolved peaks at  $0.0$  and  $-1.5$  ppm [10]. The corresponding  $^1\text{H}$  MAS spectrum reported by Yesinowski and Eckert shows two resonances at  $13.6$  and  $16.2$  ppm. Accordingly, we observe a set of cross peaks, marked with a rectangle in Fig. 6, between these  $^1\text{H}$  and  $^{31}\text{P}$  signals in our HETCOR spectrum. In comparison, the HETCOR spectrum of OCP reported by Santos and coworkers has rather poor resolution in the  $^{31}\text{P}$  dimension [8], which is presumably due to the low field and slow MAS conditions employed in their experiment.

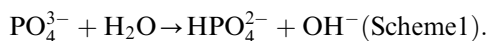
#### 4. Discussion

OCP is a metastable compound and it will transform to HAP or monetite under hydrolysis or dehydration [3]. Conventionally, OCP can be prepared by a number of methods such as the hydrolysis of brushite or by mixing suitable calcium and phosphate salts at adjusted pH condition [18]. It has been recently shown that hydrolysis of urea will produce a uniform pH change in the bulk solution so that the precipitation of calcium phosphates will become more homogeneous [19,20].

The SEM image (Fig. 2b) shows that the morphology of the OCP crystal prepared in this fashion is indeed more uniform than those prepared by other methods (data not shown).

Our  $^{31}\text{P}$  double quantum and  $^{31}\text{P}\{^1\text{H}\}$  HETCOR results provide unequivocal assignments of the  $^{31}\text{P}$  MAS spectrum, and yet it is surprising that the intensity ratio of the  $^{31}\text{P}$  peaks is not consistent with what we expected from the crystallographic data (Fig. 3). According to our assignment, the peaks positioned at  $-0.2$  (P5, P6),  $2.0$  (P3),  $3.3$  (P2, P4) and  $3.7$  (P1) ppm should have an intensity ratio of  $2:1:2:1$  but what has been measured for our OCP sample is  $3:1:1:1$ . While one may argue that the presence of monetite in our sample makes the peak at  $-0.2$  ppm more intense than expected, it is not conceivable that the amount of monetite could account for the exceedingly large population of  $\text{HPO}_4^{2-}$  [3]. In addition, the intensity of the resonance at  $3.3$  ppm indicates that the populations of P2 and P4 are significantly underrepresented in our OCP sample. To investigate the possibility of  $\text{PO}_4^{3-}$  substitution by  $\text{CO}_3^{2-}$  or  $\text{HCO}_3^-$  ions, we have conducted a  $^{13}\text{C}$  Bloch decay measurement (10 kHz MAS spinning; recycle delay 300 s; number of scans 226). However, we did not observe any  $\text{CO}_3^{2-}$  or  $\text{HCO}_3^-$  signals (ca. 160 ppm) [21,22] except those arising from the Teflon spacer (111 ppm). Therefore, it is unlikely that substantial portion of the  $\text{PO}_4^{3-}$  sites is substituted by these ions. To rationalize the  $^{31}\text{P}$  NMR peak intensity ratio we postulate that some of the  $\text{PO}_4^{3-}$  groups at the P2 and P4 sites are involved in the

following transformation:



This postulation is supported by our HETCOR result that the  $\text{PO}_4^{3-}$  groups at P2 and P4 are in close vicinity of the water molecule whose oxygen atom corresponds closely to the OH site in HAP (Table 1). Previously it has been postulated that the formation of OH group is occurred by the chemical exchange process between the P6 ( $\text{HPO}_4^{2-}$ ) and the water molecule at the OH site [1]:



In view of the fact that the phosphorous groups at P2, P4, P6 are at about the same distance to the OH site (see Table 1), the formation of OH group in our OCP sample may occur via both schemes. On the other hand, P1 is rather isolated from the water molecules and P3 is hydrogen bonded to one of the  $\text{HPO}_4^{2-}$  groups [1]. Therefore, both P1 and P3 are not involved in any chemical exchange processes.

In the literature, a recent  $^{31}\text{P}$  MAS spectrum measured under similar conditions is very similar to ours except that the peak intensity of the P2/P4 site is significantly higher than that of ours [13]. Clearly, the extent of  $\text{PO}_4^{3-}$  hydrolysis (scheme 1) is largely dependent on the preparative conditions. Although it is very difficult to prepare OCP in pure form,  $^{31}\text{P}$  NMR remains an effective analytical technique to study the structure of this mixed phase system. A systematic study of OCP structures prepared under different conditions will be the subject of a forthcoming article.

## 5. Conclusion

The high-resolution  $^{31}\text{P}$  spectrum of OCP has been assigned based on  $^{31}\text{P}$  double-quantum and  $^{31}\text{P}\{^1\text{H}\}$  HETCOR experiments. The  $^{31}\text{P}$  peaks at -0.2, 2.0, 3.3 and 3.7 ppm are assigned to P5/P6, P3, P2/P4 and P1, respectively. This assignment is consistent with all the earlier works in the literature. Our data reveal that substantial amount of the  $\text{PO}_4^{3-}$  groups at the P2 and P4 sites have been transformed to  $\text{HPO}_4^{2-}$  in our OCP sample. Overall, our results have provided a useful basis for the identification of OCP as well as the study of OCP to HAP transformation.

## Acknowledgments

This work was supported by a grant from the National Science Council under the contract number NSC 92-2119-M-002-025.

## References

- [1] M. Mathew, W.E. Brown, L.W. Schroeder, B. Dickens, *J. Cryst. Spec. Res.* 18 (1988) 235–250.
- [2] S.V. Dorozhkin, M. Epple, *Angew. Chem. Int. Ed.* 41 (2002) 3130–3146.
- [3] W.E. Brown, J.P. Smith, J.R. Lehr, A.W. Frazier, *Nature* 196 (1962) 1050–1055.
- [4] P. Bodier-Houlle, P. Steuer, J.-C. Voegel, F.J.G. Cuisinier, *Acta Cryst. D* 54 (1998) 1377–1381.
- [5] W.E. Brown, L.W. Schroeder, J.S. Ferris, *J. Phys. Chem.* 83 (1979) 1385–1388.
- [6] W.E. Brown, *Nature* 196 (1962) 1048–1050.
- [7] J.P. Yesinowski, H. Eckert, *J. Am. Chem. Soc.* 109 (1987) 6274–6282.
- [8] R.A. Santos, R.A. Wind, C.E. Bronnimann, *J. Magn. Reson. Ser. B* 105 (1994) 183–187.
- [9] A. Kafilak-Hachulska, A. Samoson, W. Kolodziejski, *Calcif. Tissue Int.* 73 (2003) 476–486.
- [10] W.P. Rothwell, J.S. Waugh, J.P. Yesinowski, *J. Am. Chem. Soc.* 102 (1980) 2637–2643.
- [11] W.P. Aue, A.H. Roufosse, M.J. Glimcher, R.G. Griffin, *Biochemistry* 23 (1984) 6110–6114.
- [12] J.L. Miquel, L. Facchini, A.P. Legrand, C. Rey, J. Lemaitre, *Colloid Surface* 45 (1990) 427–433.
- [13] M. Iijima, D.G.A. Nelson, Y. Pan, A.T. Kreinbrink, M. Adachi, T. Goto, Y. Moriwaki, *Calcif. Tissue Int.* 59 (1996) 377–384.
- [14] G. Metz, X.L. Wu, S.O. Smith, *J. Magn. Reson. A* 110 (1994) 219–227.
- [15] M. Eden, M.H. Levitt, *J. Chem. Phys.* 111 (1999) 1511–1519.
- [16] M. Hohwy, H.J. Jakobsen, M. Eden, M.H. Levitt, N.C. Nielsen, *J. Chem. Phys.* 108 (1998) 2686–2694.
- [17] Y.K. Lee, N.D. Kurur, M. Helmle, O.G. Johannessen, N.C. Nielsen, M.H. Levitt, *Chem. Phys. Lett.* 242 (1995) 304–309.
- [18] R.Z. LeGeros, *Calcif. Tissue Int.* 37 (1985) 194–197.
- [19] K. Matsuda, Y. Kaneko, H.J. Fei, K. Fujita, S. Mitsuzawa, *Proc. Fac. Sci. Tokai Univ.* 27 (1992).
- [20] K.M. Udert, T.A. Larsen, M. Biebow, W. Gujer, *Water Res.* 37 (2003) 2571–2582.
- [21] D. Stueber, A.M. Orendt, J.C. Facelli, R.W. Parry, D.M. Grant, *Solid State Nucl. Magn. Reson.* 22 (2002) 29–49.
- [22] K. Beshah, C. Rey, M.J. Glimcher, M. Shimizu, R.G. Griffin, *J. Solid State Chem.* 84 (1990).